HIGH-Q, TUNABLE-GAP MEMS VARIABLE CAPACITOR ACTUATED WITH AN ELECTRICALLY FLOATING PLATE

Hyung Suk Lee, Young Jun Yoon, Dong-Hoon Choi, and Jun-Bo Yoon
School of Electrical Engineering and Computer Science,
Korea Advanced Institute of Science and Technology (KAIST),
373-1 Guseong-dong, Yuseong-gu, Daejeon, 305-701, Republic of Korea

ABSTRACT

We proposed and developed a new MEMS variable capacitor that resembles the tunable-gap capacitor at first glance, but provides much better *Q*-factor thanks to reducing series resistance by the elimination of mechanical spring in the RF signal pathway using a new actuation method of moving electrically floating plate. The fabricated variable capacitor showed almost 200% increment of *Q*-factor from the conventional tunable-gap capacitor. In addition, a variable capacitor array connected in parallel with four capacitors for larger capacitance was fabricated and measured. We achieved a tuning ratio of 41% and *Q*-factor of 34.9 at 5GHz for the single capacitor and the tuning ratio of 29% and *Q*-factor of 39.8 at 1GHz for the capacitor array.

1. INTRODUCTION

Recently, RF variable capacitors have been required in the implementation of on-chip, high-*Q LC* tanks for use in tunable filters, voltage controlled oscillators (VCO's), tunable matching networks, and loaded-line phase shifters. Traditional semiconductor variable capacitors include varactor diodes and MOS capacitors, which suffer from excessive semiconductor series resistive losses and parasitic capacitance to the substrate resulting in low unloaded *Q*-factors. However, MEMS variable capacitors often use highly conductive metal layers, thus offering substantial improvement of the series resistive losses. To date, MEMS variable capacitors have been actively researched for achieving higher *Q*-factor, tuning ratio, and self resonant frequency than those of the semiconductor on-chip variable capacitors [1].

MEMS variable capacitors can be classified into three categories based upon a simple two-plates capacitance equation: changing the dielectric constant (ε) in between two plates [2]; tuning the gap (d) between two plates [3-5]; and varying the overlap area (A) between two comb structures [6]. Despite the use of highly conductive materials such as metal in their construction, the *Q*-factor of MEMS variable capacitors to date is still limited by losses arising from the finite resistance of their suspension beams (i.e. mechanical spring) in the RF signal pathway, which often must be made long and thin to attain stiffness values low enough to insure sufficiently low actuation voltages [4]. In effect, traditional MEMS variable capacitor designs clearly exhibit a *Q*-factor versus actuation voltage trade-off. On the other hand, the tunable-dielectric method showed higher *Q*-factor than the others so far by the elimination of mechanical spring in the RF signal pathway but it has complex fabrication process [2].

This work breaks the above trade-off relationship by eliminating the inevitable mechanical spring in the RF signal pathway (i.e. RF signal does not pass through the mechanical spring), and hence, allows almost 200% increment of *Q*-factor from the conventional tunable-gap capacitor.

2. OPERATIONAL PRINCIPLES

Fig. 1(a) and (b) present conceptual schematics of the conventional tunable-gap capacitor and proposed tunable-gap capacitor designs, identifying key components and specifying a preferred actuation voltage configuration and RF signal pathway. As shown in Fig. 1(a), the conventional tunable-gap capacitor needs to be applied a DC bias (as well as the RF signal) through the mechanical spring to change the capacitance by moving the suspended top plate. In this design, a long, thin, and narrow mechanical spring for lowering down the actuation voltage results in larger electrical spring resistance and lower *Q*-factor. Contrarily, the DC bias and RF signal are applied between two fixed bottom plates (not through the mechanical spring) in the proposed method as shown in Fig. 1(b). The floating top plate suspended above those two bottom plates is electrostatically pulled down to increase the capacitance when the DC bias is applied between the two bottom plates. Since the mechanical springs are decoupled from the floating top plate in the RF signal pathway, thicker floating top plate can be achieved to obtain higher *Q*-factor leaving the actuation voltage unaffected. Note that the proposed method can also be interpreted as a series connection of the two tunable-gap capacitors as shown in Fig. 1(b).

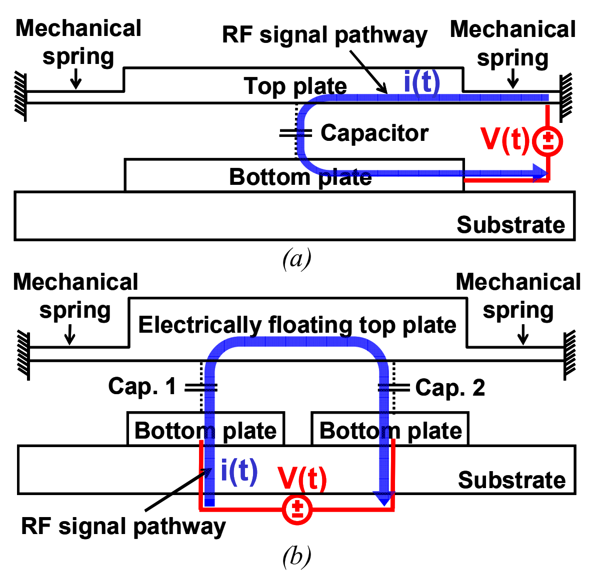

Figure 1. A schematic view of (a) conventional variable capacitor with two parallel-plates (b) proposed variable capacitor actuated with an electrically floating top plate.

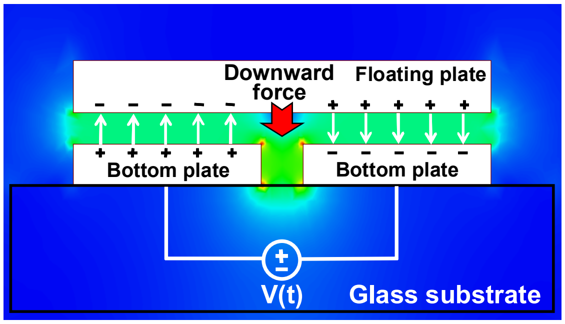

Figure 2. Electrostatic field simulation result performed by Maxwell® 2D showing E-field confinement between two fixed bottom plates and the electrically floating top plate.

Fig. 2 shows the Maxwell® simulation result displaying E-field confinement between the electrically floating plate and two bottom plates. Due to the electrically floating plate located above the bottom plates, an unbalance of the E-field distribution between above and below region of the floating plate is produced, and thus, a net downward force is induced to the floating plate; i.e. the floating plate naturally tends to be moved toward increasing the capacitance of the system. The larger DC bias is applied, the larger unbalance of E-field distribution is induced, thus the floating plate continuously moves downward until the net downward force and an elastic force of mechanical spring are in equilibrium. When the floating plate reaches two-thirds of initial gap (the same as the conventional tunable-gap capacitor) with applied bias, the floating plate shows pull-in phenomenon and attaches to the bottom plates.

3. DESIGN AND FABRICATION

Fig. 3 presents an actual structure design, consisting of two fixed bottom plates with a dielectric layer, and the electrically floating thick plate suspended above those two bottom plates, which is rigidly anchored to the substrate through thin mechanical springs.

Fig. 4 illustrates the simplified fabrication process for this work. The process begins with a glass wafer to serve as an insulating substrate. The bottom plates are formed by first evaporating 200Å/5000Å of Cr/Cu seed layer, then electroplating 2.5μm or 5μm of Cu through the patterned photoresist mold. 1000Å of SiO_2 dielectric layer is then deposited by PECVD and patterned above the bottom plates to prevent short-circuit between bottom plates and floating plate during actuation. In order to form initial gap between bottom plates and floating plate, 1.2μm-thick sacrificial photoresist is used. Next, 1000Å of Cu is evaporated above the sacrificial photoresist, and then, the floating plate and mechanical spring are electroplated through the patterned photoresist mold. In order to achieve thicker floating plate, patterning of photoresist followed by Cu electroplating only at the floating plate region is performed. All sacrificial layers including two photoresist mold for floating plate, Cu seed layer, and 1.2μm-thick sacrificial photoresist are removed sequentially and Cr seed layer is selectively etched using a $K_3Fe(CN)_6$/NaOH solution [2], which etches away Cr, but leaves Cu and SiO_2 dielectric intact, yielding the final cross-section of Fig.4(d). Finally, a critical point drying is used to release the device preventing stiction. Since we can decouple the mechanical spring from the floating plate in the RF signal pathway, thicker floating plate can be fabricated to achieve higher *Q*-factor leaving the actuation voltage unaffected, as shown in Fig. 4(c). The SEM photograph of the fabricated device with the floating plate of 400μm × 400μm in size and the initial gap of 1.2μm is shown in Fig. 5. No warping of the structure was observed and especially, the thicker floating plate and thinner mechanical spring were clearly observed as shown in the magnified inset of Fig. 5.

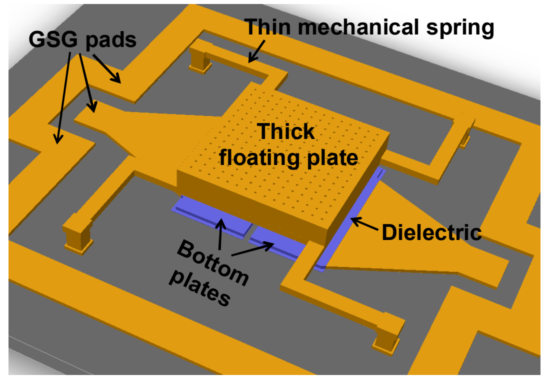

Figure 3. Actual structure design of the proposed variable capacitor.

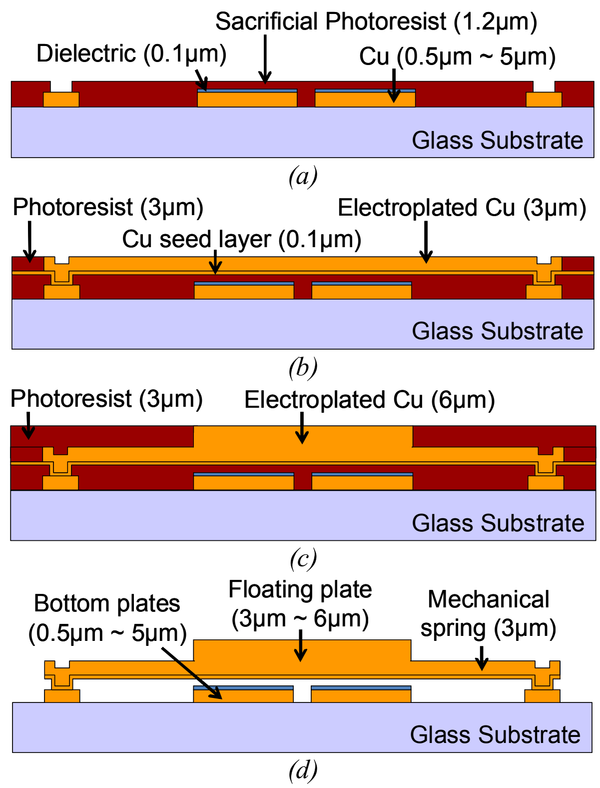

Figure 4. Simplified fabrication process (a) Deposition and patterning of the bottom plate, dielectric, and sacrificial photoresist (b) Cu seed metal deposition and patterning of the thick photoresist followed by Cu electroplating of the floating plate and mechanical spring (c) (Optional) Patterning of the thick photoresist and Cu electroplating of only the floating plate area (d) Releasing by sacrificial layer etching.

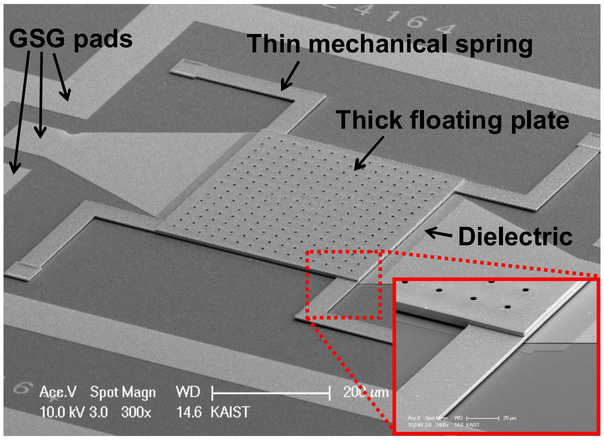

Figure 5. SEM photograph of the fabricated variable capacitor.

4. RESULT AND DISCUSSION

In order to characterize the device performances, RF measurements from 1 to 10GHz were made using an HP8510 s-parameter network analyzer together with GSG-tipped GGB microwave probes and short-open-load-through (SOLT) calibration.

Fig. 6 presents measured RF performance of the type 1 capacitor for 5GHz applications, where the specification is described in the table of Fig 7.(b), showing the maximum tuning ratio of 41% from 0V to 5.5V (the expected pull-in voltage of 5.6V) at 5GHz and *Q*-factor of 27.1 when biased with 0V, 26.7 when biased with 5V, respectively at 5GHz. Regardless of the applied biases, *Q*-factors were almost the same at all frequency range from 1GHz to 10GHz.

Fig 7. compares measured *Q*-factors between the conventional tunable-gap capacitor designed to have the same initial capacitance with the same initial gap and the proposed variable capacitors with different bottom and floating plate thicknesses. Fig. 7(a) depicts the *Q*-factor vs. frequency for the fabricated devices when biased with 0V and table in Fig. 7(b) summarizes the device specifications and performance in respect of *Q*-factor. The proposed variable capacitor with thicker bottom plates and floating plate showed almost 200% increment (i.e. 3 times higher) in *Q*-factor at 5GHz compared with the conventional type. The thicker bottom plates and floating plate were provided, the higher *Q*-factor was obtained. In addition, it was observed that the thickness of bottom plates is more dominant factor than that of the floating plate, which is associated with the skin depth of RF signal that one needs the copper thickness over 5μm at 1GHz [7]. Note that all fabricated devices showed average pull-in voltage of 5.5V with standard deviation of 7% and expected to have self resonant frequency over 10GHz. Furthermore, some of the proposed variable capacitors show the maximum *Q*-factor exceeding 300 at 1GHz, on the contrary, the maximum *Q*-factor of about 70 at 1GHz for conventional tunable-gap capacitor.

In order to achieve larger capacitance, an array of the four proposed variable capacitors which were connected in parallel was fabricated and measured as shown in Fig 8. It shows an initial capacitance of 1.52pF, the maximum tuning ratio of 29% from 0V to 3.3V (the expected pull-in voltage of

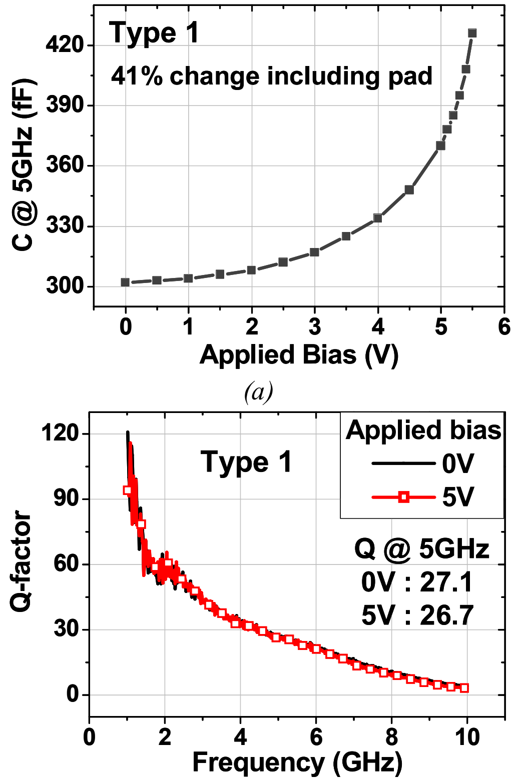

(b)

Figure 6. Measured RF characteristics of the fabricated variable capacitor (a) Capacitance at 5GHz vs. applied bias (b) Q-factor vs. frequency.

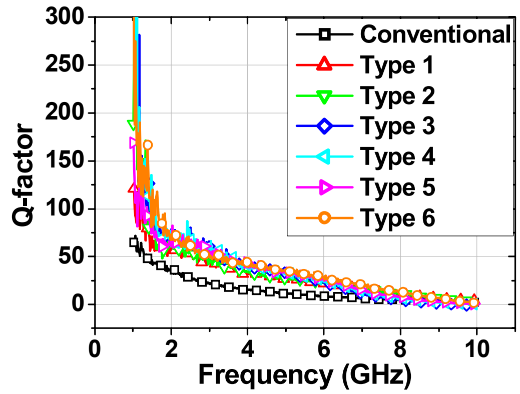

(a)

Type	Bottom plate thickness	Spring thickness	Floating plate thickness	*Q*-factor @ 5GHz	*Q*-factor improvement
Conventional	0.5 μm	3 μm	3 μm	11.7	-
Type 1	0.5 μm	3 μm	3 μm	27.1	132 %
Type 2	0.5 μm	3 μm	6 μm	28.2	141 %
Type 3	2.5 μm	3 μm	3 μm	32.7	179 %
Type 4	2.5 μm	3 μm	6 μm	33.2	184 %
Type 5	5 μm	3 μm	3 μm	35.0	199 %
Type 6	5 μm	3 μm	6 μm	34.9	198 %

(b)

Figure 7. Comparison of Q-factors between the conventional variable capacitor and the proposed variable capacitors with different bottom and floating plate thicknesses. (a) Q-factor vs. frequency (b) Table of the device specifications and performance.

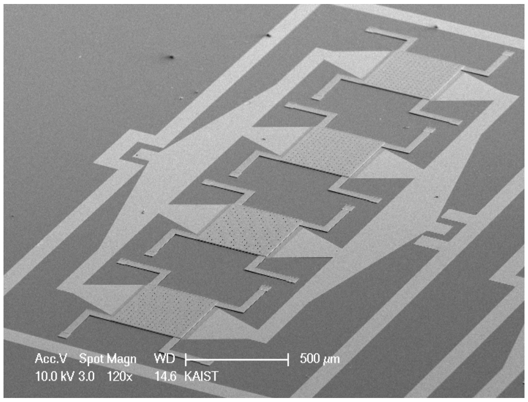

(a)

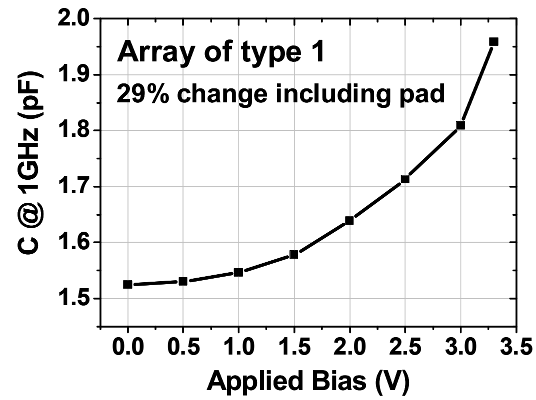

(b)

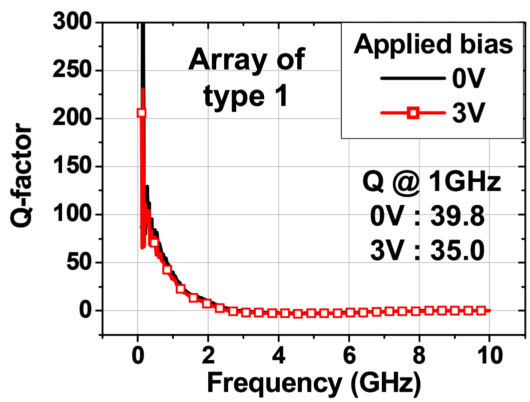

(c)

Figure 8. Measured RF characteristics of the variable capacitor array connected in parallel with four capacitors (a) SEM photograph (b) Capacitance at 1GHz vs. applied bias (c) Q-factor vs. frequency.

3.4V) at 1GHz, and *Q*-factor of 39.8 when biased with 0V, 35.0 when biased with 3V, respectively at 1GHz. The measured self resonant frequency was 3GHz, which is smaller than that of single variable capacitor, and it was originated from the inductive elements of parallel connection lines.

5. CONCLUSIONS

A new MEMS variable capacitor actuated with the electrically floating plate has been proposed and successfully demonstrated in this work. The proposed variable capacitor showed better *Q*-factor performance than that of the conventional tunable-gap capacitor by means of eliminating the electrical series resistance of mechanical spring in the RF signal pathway. The new actuation mechanism of moving electrically floating plate can also be applied to other MEMS applications. When combined with on-chip high-*Q* inductors, these capacitors are expected to be useful for high performance RF tunable devices.

REFERENCES

[1] H. A. C. Tilmans, W. De Raedt and E. Beyne, "MEMS for wireless communications: from RF-MEMS components to RF-MEMS-SiP," *J. Micromech. Microeng.*, vol. 13, pp. 139-163, 2003.

[2] J.-B. Yoon and C. T.-C. Nguyen, "A high-Q tunable micromechanical capacitor with movable dielectric for RF applications," in *IEEE International Electron Devices Meeting*, Dec. 11-13, 2000, pp. 489-492.

[3] D. J. Young and B. E. Boser, "A micromachined variable capacitor for monolithic low-noise VCOs," in *IEEE Solid-State Sensor and Actuator Workshop Dig.*, June 2-6, 1996, pp. 86-89.

[4] A. Dec and K. Suyama, "Micromachined electro-mechanically tunable capacitors and their applications to RF IC's," *IEEE Trans. Microwave Theory and Tech.*, vol. 46, pp. 2587-2596, 1998.

[5] A. Dec and K. Suyama, "Microwave MEMS-based voltage-controlled oscillators," *IEEE Trans. Microwave Theory and Tech.*, vol. 48, pp. 1943-1949, 2000.

[6] J. J. Yao, S. T. Park and J. DeNatale," High tuning ratio MEMS based tunable capacitors for RF communications applications," in *IEEE Solid-State Sensor and Actuator Workshop Dig.*, June 8-11, 1998, pp. 124-127.

[7] G. M. Rebeiz, *RF MEMS Theory, design, and technology*, John Wiley and Sons, Inc., New Jersey, 2003.